Flexural wave propagation in single-walled carbon nanotubes

Lifeng Wang and Haiyan Hu*
Institute of Vibration Engineering Research, Nanjing University of Aeronautics and Astronautics, 210016, Nanjing, China
(Received 26 October 2004; revised manuscript received 18 January 2005; published 23 May 2005)

The paper presents the study on the flexural wave propagation in a single-walled carbon nanotube through the use of the continuum mechanics and the molecular dynamics simulation based on the Terroff-Brenner potential. The study focuses on the wave dispersion caused not only by the rotary inertia and the shear deformation in the model of a traditional Timoshenko beam, but also by the nonlocal elasticity characterizing the microstructure of carbon nanotube in a wide frequency range up to THz. For this purpose, the paper starts with the dynamic equation of a generalized Timoshenko beam made of the nonlocal elastic material, and then gives the dispersion relations of the flexural wave in the nonlocal elastic Timoshenko beam, the traditional Timoshenko beam and the Euler beam, respectively. Afterwards, it presents the molecular dynamics simulations for the flexural wave propagation in an armchair (5,5) and an armchair (10,10) single-walled carbon nanotubes for a wide range of wave numbers. The simulation results show that the Euler beam holds for describing the dispersion of flexural waves in the two single-walled carbon nanotubes only when the wave number is small. The Timoshenko beam provides a better prediction for the dispersion of flexural waves in the two single-walled carbon nanotubes when the wave number becomes a little bit large. Only the nonlocal elastic Timoshenko beam is able to predict the decrease of phase velocity when the wave number is so large that the microstructure of carbon nanotubes has a significant influence on the flexural wave dispersion.

DOI: 10.1103/PhysRevB.71.195412 PACS number(s): 81.07.De, 62.25.+g, 62.30.+d

I. INTRODUCTION

Interest in carbon nanotubes has kept growing since their discovery by Iijima.[1] Recent studies have indicated that carbon nanotubes exhibit superior mechanical and electronic properties over any known materials and hold substantial promise for, among others, new super-strong composite materials. For instance, carbon nanotubes possess exceptionally high elastic modulus[2–6] and sustain large elastic strain and failure strain.[7–10] The mechanics of carbon nanotubes, hence, has drawn considerable attention. Numerous studies have concentrated on the static mechanical behavior, such as buckling, of carbon nanotubes by using the models of elastic beams and shells, and even those of nonlocal elastic beams and shells.[11,12] Meanwhile, several research teams have implemented the model of elastic beams to study the dynamic problems, such as the vibration[13–15] and the wave propagation,[16–18] of carbon nanotubes. For example, Yoon *et al.* studied the flexural wave propagation in a multi-walled carbon nanotube based on the model of Timoshenko beam with the rotary inertia and the shear deformation taken into account.[18] To the best knowledge of the authors, however, neither experiments nor numerical simulations have been available for the validation of beam models in studying the flexural wave propagation in any carbon nanotube from the viewpoint of continuum mechanics. Furthermore, little is known about the effect of the microstructure, if any, on the flexural wave propagation in a carbon nanotube.

The primary objective of this study is to check the validity of the beam model in studying the flexural waves, simulated by the molecular dynamics, in a single-walled carbon nanotube. In the preliminary stage of this study, the molecular dynamics simulation showed that the microstructure of a carbon nanotube had a significant influence on the dispersion of flexural waves of high frequency such that no traditional beam models, neither the Euler beam nor the Timoshenko beam, could predict the decrease in the phase velocity. Thus, there is a need to study the dispersion of flexural waves in single-walled carbon nanotubes based on the model of nonlocal continuum mechanics so as to take the effect of the microstructure of single-walled carbon nanotubes on the wave dispersion into consideration.

For this purpose, the dynamic equation is established for a nonlocal elastic Timoshenko beam, which takes not only the rotary inertia and the shear deformation, but also the second-order gradient of strain which characterizes the microstructure of carbon nanotubes, into account in Sec. II. In Sec. III, the dispersion relations of flexural waves are derived for the nonlocal elastic Timoshenko beam, the traditional Timoshenko beam, and the Euler beam. Afterwards, the model of molecular dynamics is outlined in Sec. IV for the single-walled carbon nanotubes. In Sec. V, a comparison is made between the theoretical results of beam models and those simulated by the molecular dynamics for the propagation of flexural waves in two single-walled carbon nanotubes. Finally, some concluding remarks are made in Sec. VI.

II. MODEL OF A NONLOCAL ELASTIC TIMOSHENKO BEAM

This section starts with the dynamic equation of a nonlocal elastic Timoshenko beam of infinite length and uniform cross section placed along direction x in the frame of coordinates (x,y,z), with $w(x,t)$ being the displacement of section x of the beam in direction y at the moment t.

In order to describe the effect of the microstructure of carbon nanotubes on their mechanical properties, it is assumed that the beam of concern is made of the nonlocal elastic material, where the stress state at a given reference

point depends not only on the strain of this point, but also on the higher-order gradient of strain so as to take the influence of the long range forces of all other atoms into account. The simplest constitutive law to characterize the nonlocal elastic material in the one-dimensional case reads

$$\sigma_x = E\left(\varepsilon_x + r^2\frac{\partial^2\varepsilon_x}{\partial x^2}\right), \tag{1}$$

where E represents Young's modulus and ε_x the axial strain. As studied in Askes *et al.*[19] (see Appendix), r is a material parameter to reflect the influence of the microstructure on the stress in the nonlocal elastic material and yields

$$r = \frac{d}{\sqrt{12}}, \tag{2}$$

where d, referred to as the interparticle distance, is the axial distance between two rings of particles in the material. For the armchair single-walled carbon nanotube, d is just the axial distance between two rings of carbon atoms.

To establish the dynamic equation of the beam, it is necessary to determine the bending moment M, which reads

$$M = \int_A y\sigma_x dA, \tag{3}$$

where A represents the cross section area of the beam, σ_x the axial stress, and y the distance from the centerline of the cross section. It is well known from the theory of beams that the axial strain yields

$$\varepsilon_x = \frac{y}{\rho'}, \tag{4}$$

where ρ' is the radius of curvature of beam. Let φ denote the slope of the deflection curve when the shearing force is neglected and s denote the coordinate along the deflection curve of the beam. Then the assumption upon the small deflection of beam gives

$$\frac{1}{\rho'} = \frac{\partial\varphi}{\partial x}\frac{\partial x}{\partial s} \approx \frac{\partial\varphi}{\partial x}. \tag{5}$$

Substituting Eqs. (4) and (5) into Eqs. (1) and (3) gives the following relation between bending moment M and the curvature and its second derivative when the shearing force is neglected:

$$M = EI\left(\frac{\partial\varphi}{\partial x} + r^2\frac{\partial^3\varphi}{\partial x^3}\right), \tag{6}$$

where $I=\int y^2 dA$ represents the moment of inertia for the cross section.

To determine the shear force on the beam, let γ be the angle of shear at the neutral axial in the same cross section. Then, it is easy to see the total slope

$$\frac{\partial w}{\partial x} = \varphi - \gamma. \tag{7}$$

For the torsional problem of one dimension, the constitutive law of the nonlocal elastic material reads

$$\tau = G\left(\gamma + r^2\frac{\partial^2\gamma}{\partial x^2}\right), \tag{8}$$

where τ is the shear stress and G is the shear modulus. Then, the shear force Q on the cross section becomes

$$Q = \beta AG\left[\left(\varphi - \frac{\partial w}{\partial x}\right) + r^2\left(\frac{\partial^2\varphi}{\partial x^2} - \frac{\partial^3 w}{\partial x^3}\right)\right], \tag{9}$$

where β is the form factor of shear depending on the shape of the cross section, and $\beta=0.5$ holds for the circular tube of the thin wall.[20]

Now, it is straightforward to write out the dynamic equation for the beam element of length dx subject to bending M and shear force Q as follows:

$$\rho A\frac{\partial^2 w}{\partial t^2}dx + \frac{\partial Q}{\partial x}dx = 0,$$

$$\rho I\frac{\partial^2\varphi}{\partial t^2}dx + Qdx - \frac{\partial M}{\partial x}dx = 0. \tag{10}$$

Substituting Eqs. (6) and (9) into Eq. (10) yields the following coupled dynamic equation for the deflection and the slop of nonlocal elastic Timoshenko beam

$$\rho\frac{\partial^2 w}{\partial t^2} + \beta G\left[\left(\frac{\partial\varphi}{\partial x} - \frac{\partial^2 w}{\partial x^2}\right) + r^2\left(\frac{\partial^3\varphi}{\partial x^3} - \frac{\partial^4 w}{\partial x^4}\right)\right] = 0,$$

$$\rho I\frac{\partial^2\varphi}{\partial t^2} + \beta AG\left[\left(\varphi - \frac{\partial w}{\partial x}\right) + r^2\left(\frac{\partial^2\varphi}{\partial x^2} - \frac{\partial^3 w}{\partial x^3}\right)\right] - EI\left(\frac{\partial^2\varphi}{\partial x^2} + r^2\frac{\partial^4\varphi}{\partial x^4}\right) = 0. \tag{11}$$

III. FLEXURAL WAVE DISPERSION IN DIFFERENT BEAM MODELS

To study the flexural wave propagation in an infinitely long beam, let the dynamic deflection and slope be given by

$$w(x,t) = \hat{w}e^{ik(x-ct)}, \quad \varphi(x,t) = \hat{\varphi}e^{ik(x-ct)}, \tag{12}$$

where $i\equiv\sqrt{-1}$, $\hat{w}$ represents the amplitude of deflection of the beam, and $\hat{\varphi}$ represents the amplitude of the slope of the beam due to bending deformation alone. In addition, c is the phase velocity of wave, and k is the wave number related to the wavelength λ via $\lambda k=2\pi$. Substituting Eq. (12) into Eq. (11) yields

$$(-i\beta AGk + i\beta AGr^2k^3)\hat{w} + (-\rho Ik^2c^2 + \beta AG - \beta AGr^2k^2 + EIk^2 - EIr^2k^4)\hat{\varphi} = 0,$$

$$(-\rho k^2c^2 + \beta Gk^2 - \beta Gr^2k^4)\hat{w} + (i\beta Gk - i\beta Gr^2k^3)\hat{\varphi} = 0. \tag{13}$$

From the fact that there exists at least one nonzero solution $(\hat{w},\hat{\varphi})$ of Eq. (13), one arrives at

$$\frac{\rho^2 I}{\beta G}k^2c^4 - \left[\rho A + \rho I\left(1 + \frac{E}{\beta G}\right)k^2\right](1 - r^2k^2)c^2 + EIk^2(1 - r^2k^2)^2 = 0. \quad (14)$$

Solving Eq. (14) for the phase velocity c gives two branches of wave dispersion relation,

$$c = \sqrt{\frac{-b_1 \pm \sqrt{b_1^2 - 4a_1c_1}}{2a_1}}, \quad (15)$$

where $a_1 = \rho^2 Ik^2/\beta G$, $b_1 = [\rho A + \rho I(1 + E/\beta G)k^2](r^2k^2 - 1)$, and $c_1 = EIk^2(1 - r^2k^2)^2$. Here, the lower branch represents the dispersion relation of the flexural wave, and the upper branch determines the dispersion relation of the transverse shearing out of interest.

If $r = 0$, Eq. (11) leads to

$$\rho A\frac{\partial^2 w(x,t)}{\partial t^2} + EI\frac{\partial^4 w(x,t)}{\partial x^4} - \rho I\left(1 + \frac{E}{\beta G}\right)\frac{\partial^4 w(x,t)}{\partial x^2 \partial t^2} + \frac{\rho^2 I}{\beta G}\frac{\partial^4 w(x,t)}{\partial t^4} = 0. \quad (16)$$

This is the dynamic equation of a traditional Timoshenko beam.[21] In this case, the relation of wave dispersion takes the form of Eq. (15), but with $a_1 = \rho^2 Ik^2/\beta G$, $b_1 = -[\rho A + \rho I(1 + E/\beta G)k^2]$, and $c_1 = EIk^2$.

If neither the rotary inertial nor the shear deformation is taken into account, Eq. (11) leads to the dynamic equation of a nonlocal elastic Euler beam as follows:

$$\rho A\frac{\partial^2 w(x,t)}{\partial t^2} + EI\left[\frac{\partial^4 w(x,t)}{\partial x^4} + r^2\frac{\partial^6 w(x,t)}{\partial x^6}\right] = 0. \quad (17)$$

The condition of nonzero solution $\hat{w}$ of Eq. (17) gives the dispersion relation

$$c = k\sqrt{\frac{EI}{\rho A}(1 - r^2k^2)}. \quad (18)$$

In this case, $r = 0$ results in the dispersion relation in the traditional Euler beam

$$c = k\sqrt{\frac{EI}{\rho A}}. \quad (19)$$

IV. MOLECULAR DYNAMICS MODEL FOR CARBON NANOTUBES

In order to check the applicability of the above dispersion relations given by different beam models to the single-walled carbon nanotubes, this section presents the model of molecular dynamics simulations for two single-walled carbon nanotubes. They both are 29.5 nm long, but one is an armchair (5,5) carbon nanotube and the other is an armchair (10,10) carbon nanotube, respectively.

In the corresponding molecular dynamics models, the interatomic interactions are described by the Tersoff-Brenner potential,[22] which has been proved applicable to the description of mechanical properties of single-walled carbon nanotubes. The structure of the Tersoff-Brenner potential is as follows:

$$V(r_{ij}) \equiv \sum_i \sum_{j(>i)} [V_R(r_{ij}) - \overline{B}_{ij}V_A(r_{ij})], \quad (20)$$

where r_{ij} is the distance from atom i to atom j, and $V_R(r_{ij})$ and $V_A(r_{ij})$ are the repulsive and attractive terms given by

$$V_R(r_{ij}) \equiv f_{ij}(r_{ij})\frac{D_{ij}}{S_{ij} - 1}\exp[-\sqrt{2S_{ij}}\beta_{ij}(r - r_0)], \quad (21a)$$

$$V_A(r_{ij}) \equiv f_{ij}(r_{ij})\frac{S_{ij}D_{ij}}{S_{ij} - 1}\exp[-\sqrt{2/S_{ij}}\beta_{ij}(r - r_0)]. \quad (21b)$$

Here $S_{ij} = 1.29$, $D_{ij} = 6.325$ eV, $\beta_{ij} = 15$ nm^{-1}, $r_0 = 0.1315$ nm, f_{ij}, D_{ij}, S_{ij}, β_{ij} are scalars, and $f_{ij}(r_{ij})$ is a switch function used to confine the pair potential in a neighborhood with radius of r_2 as follows,

$$f_{ij}(r_{ij}) \equiv \begin{cases} 1, & r_{ij} < r_1, \\ \frac{1}{2}\left[1 + \cos\left(\frac{\pi(r_{ij} - r_1)}{r_2 - r_1}\right)\right], & r_1 \leqslant r_{ij} \leqslant r_2, \\ 0, & r_{ij} > r_2, \end{cases} \quad (21c)$$

where $r_1 = 1.7$ Å and $r_2 = 2.0$ Å. In Eq. (20), $\overline{B}_{ij}$ reads

$$\overline{B}_{ij} \equiv \tfrac{1}{2}(b_{ij} + b_{ji}), \quad (21d)$$

$$b_{ij} \equiv \left(1 + \sum_{k \neq i,j} G(\theta_{jik})f_{ik}(r_{ik})\right)^{-\delta},$$

$$b_{ji} \equiv \left(1 + \sum_{k \neq i,j} G(\theta_{ijk})f_{jk}(r_{jk})\right)^{-\delta}, \quad (21e)$$

$$G(\theta_{ijk}) \equiv a_0\left(1 + \frac{c_0^2}{d_0^2} - \frac{c_0^2}{d_0^2 + (1 + \cos\theta_{ijk})^2}\right), \quad (21f)$$

where θ_{ijk} is the angle between bonds i-j and i-k, $\delta = 0.80469$, $a_0 = 0.011\,304$, $c_0 = 19$, and $d_0 = 2.5$. In addition, the C—C bond length in the model is 0.142 nm.

V. FLEXURAL WAVE PROPAGATION IN SINGLE-WALLED CARBON NANOTUBES

To predict the flexural wave dispersion from the theoretical results in Sec. III, it is necessary to know Young's modulus E and the shear modulus G, or Poisson's ratio ν. The previous studies based on the Tersoff-Brenner potential gave a great variety of Young's moduli of single-walled carbon nanotubes from the simulated tests of axial tension and compression. When the thickness of the wall was chosen as 0.34 nm, for example, 1.07 TPa was reported by Yakobson *et al.*,[7] 0.8 TPa by Cornwell and Wille,[23] and 0.44–0.50 TPa by Halicioglu.[24] Meanwhile, the Young's modulus determined by Zhang *et al.*[25] on the basis of the nanoscale continuum mechanics was only 0.475 TPa when the first set of

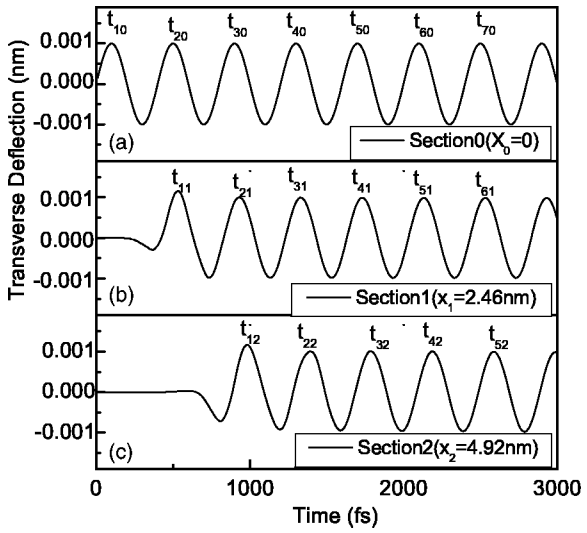

FIG. 1. The time histories of the deflection of different sections of the armchair (5,5) carbon nanotube, where subscripts i and j in t_{ij} represent the number of the wave peak and the number of the section, respectively. (a) The sinusoidal wave of period $T=400$ fs input at section 0. (b) The deflection of section 1, 2.46 nm ahead of section 0. (c) The deflection of section 2, 4.92 nm ahead of section 0.

parameters in the Tersoff-Brenner potential[22] was used. Hence, it becomes necessary to compute Young's modules and Poisson's ratio again from the above molecular dynamics model for the single-walled carbon nanotubes under the static loading.

For the same thickness of the wall, the Young's modulus that we computed by using the first set of parameters in the Tersoff-Brenner potential[22] was 0.46 TPa for the armchair (5,5) carbon nanotube and 0.47 TPa for the armchair (10,10) carbon nanotube from the molecular dynamics simulation for the test of axial tension. Furthermore, the simulated test of pure bending that we did gave the product of effective Young's modulus $E=0.39$ TPa and Poisson's ratio $\nu=0.22$ for the armchair (5,5) carbon nanotube, and $E=0.45$ TPa and $\nu=0.20$ for the armchair (10,10) carbon nanotube. In the use of theoretical results in Sec. III, Young's moduli and Poisson's ratios obtained from the simulated test of pure bending for those two carbon nanotubes were used. In addition, Eq. (2) gives $r=0.0355$ nm when the axial distance between two rings of atoms reads $d=0.123$ nm. For the single-walled carbon nanotubes, the wall thickness is $h=0.34$ nm and the mass density of the carbon nanotubes is $\rho=2237$ kg m^{-3}.

It is quite straightforward to determine the phase velocity and the wave number from the flexural vibration, simulated by using molecular dynamics, of two arbitrary sections of a carbon nanotube. As an example, the end atoms denoted by section 0 at $x_0=0$ of the armchair (5,5) carbon nanotube was assumed to be subject to the harmonic deflection of period $T=400$ fs as shown in Fig. 1(a). The corresponding angular frequency is $\omega=2\pi/T\approx 1.57\times 10^{13}$ rad s^{-1}. The harmonic deflection was achieved by shifting the edge atoms of one end of the nanotube while the other end was kept free. Figures 1(b) and 1(c) show the flexural vibrations of section 1 at $x_1=2.46$ nm and section 2 at $x_2=4.92$ nm, respectively, of the carbon nanotube simulated by using molecular dynamics. If the transient deflection of the first two periods is neglected, the propagation duration Δt of the wave from section 1 to section 2 can be estimated as below

$$\Delta t \approx \frac{(t_{32}-t_{31})+(t_{42}-t_{41})+\cdots+(t_{n2}-t_{n1})}{n-2}. \quad (22)$$

There follow the phase velocity and wave number

$$c=\frac{x_2-x_1}{\Delta t}, \quad k=\frac{2\pi}{\lambda}=\frac{\omega T}{\lambda}=\frac{\omega}{c}. \quad (23)$$

Figures 2 and 3 illustrate the dispersion relations between the phase velocity c and the wave number k, and between the phase velocity c and wavelength λ of the flexural wave in the armchair (5,5) and (10,10) carbon nanotubes, respectively. Here, the symbol E represents the traditional Euler beam, T the traditional Timoshenko beam, NE the nonlocal elastic Euler beam, NT the nonlocal elastic Timoshenko beam, and MD the molecular dynamics simulation, respectively. In Figs. 2 and 3, when the wave number k was smaller than 1×10^9 m^{-1}, or the wavelength was $\lambda>6.28\times 10^{-9}$ m, the phase velocities given by the four beam models were close to each other, and they all could predict the result of the molecular dynamics well. The phase velocity given by the traditional Euler beam, however, was proportional to the wave number, and greatly deviated from the result of molecular dynamics when the wave number became larger than 1×10^9 m^{-1}. Almost no better than the traditional Euler beam, the result of the nonlocal elastic Euler beam greatly deviated from the result of molecular dynamics too when the wave number became large. Nevertheless, the results of both the traditional Timoshenko beam and the nonlocal elastic Timoshenko beam remained in a reasonable coincidence with the results of molecular dynamics in the middle range of wavenumber or wavelength. When the wave number k was larger than 6×10^9 m^{-1} (or the wavelength was $\lambda<1.047\times 10^{-9}$ m) for the armchair (5,5) carbon nanotube and 3×10^9 m^{-1} (or the wavelength was $\lambda<2.094\times 10^{-9}$ m) for the armchair (10,10) carbon nanotube, the phase velocity given by the molecular dynamics began to decrease, which the traditional Timoshenko beam failed to predict. However, the nonlocal elastic Timoshenko beam was able to predict the decrease of phase velocity when the wave number was so large (or the wavelength was so short) that the microstructure of the carbon nanotube significantly blocked the propagation of flexural waves.

Figure 4 shows the flexural wave propagation in the armchair (5,5) carbon nanotube, simulated by using the molecular dynamics model, at the moment of 3000 fs for four different wave periods. Obviously, the wave dispersion became more and more remarkable with a decrease in wave period. As illustrated in Fig. 4, the flexural wave of period $T<100$ fs dispersed so rapidly that it could hardly propagate in the carbon nanotube.

VI. CONCLUDING REMARKS

The paper presents a detailed study on the flexural wave dispersion in single-walled carbon nanotubes on the basis of

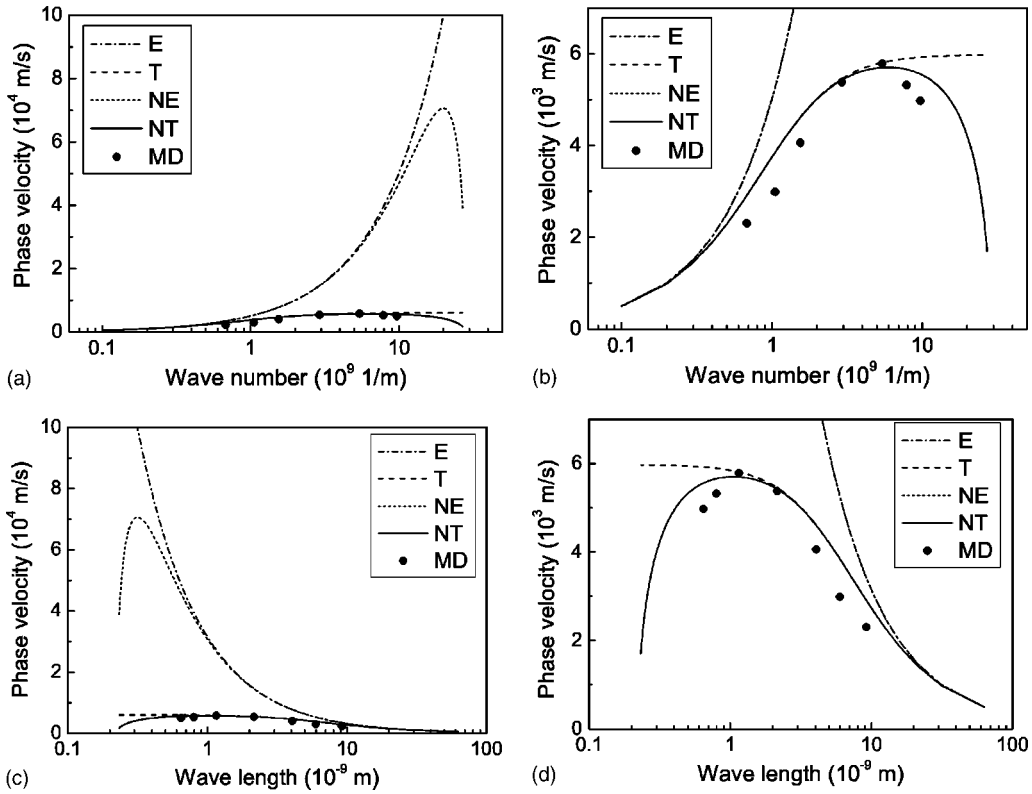

FIG. 2. The dispersion relation of the armchair (5,5) carbon nanotube. (a) The phase velocity of flexural wave versus wave number. (b) The zoom of (a); (c) The phase velocity of flexural wave versus wave length. (d) The zoom of (c).

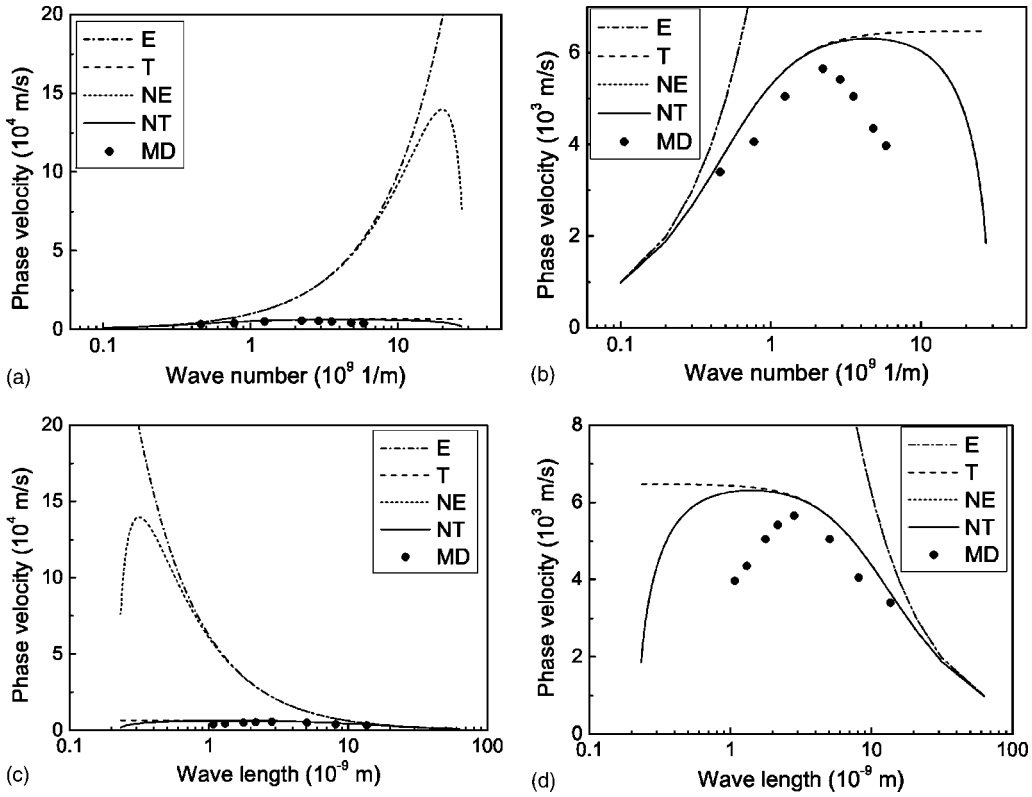

FIG. 3. The dispersion relation of the armchair (10,10) carbon nanotube. (a) The phase velocity of flexural wave versus wave number; (b) The zoom of (a); (c) The phase velocity of flexural wave versus wave length; (d) The zoom of (c).

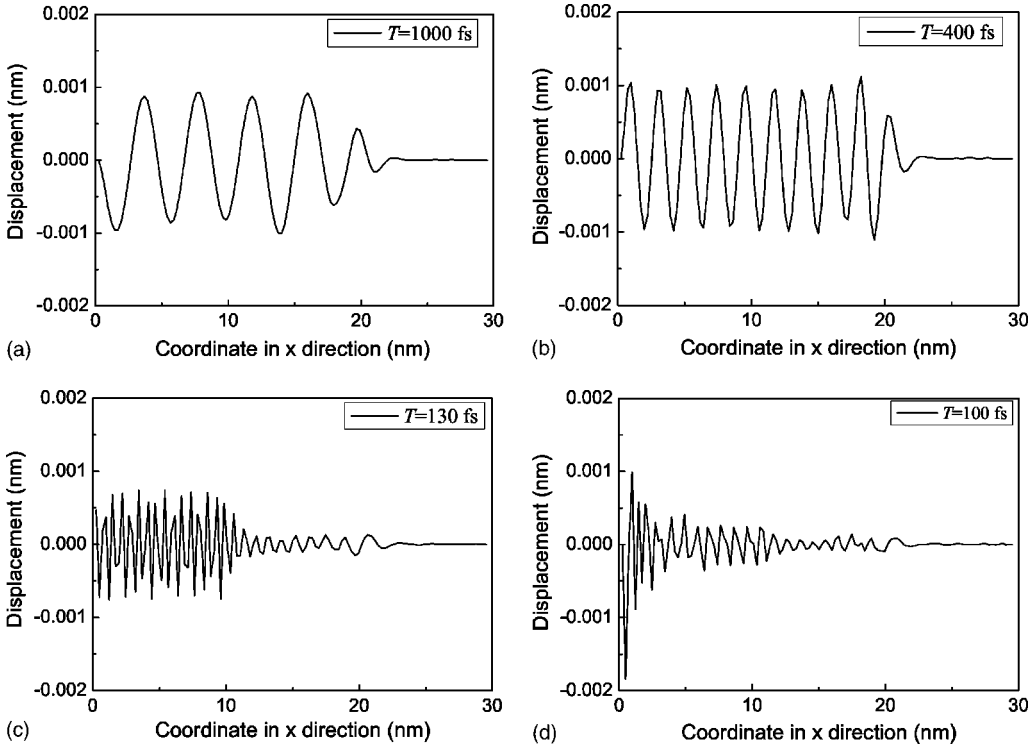

FIG. 4. The propagation of waves of periods of (a) 1000 fs, (b) 400 fs, (c) 130 fs, and (d) 100 fs, respectively, in an armchair (5,5) single-walled carbon nanotube at time step of 3000 fs by the molecular dynamics simulations.

four beam models with the help of molecular dynamics simulations for an armchair (5,5) and an armchair (10,10) carbon nanotubes, respectively, in a wide range of wave numbers. The study indicates that the traditional Timoshenko beam is able to offer a much better prediction than the traditional Euler beam and the nonlocal elastic Euler beam for the flexural wave dispersion simulated by using the molecular dynamics if the wave number is not very large. When the wave number is getting very large, the microstructure of the carbon nanotubes plays an important role in the flexural wave dispersion and significantly decreases the phase velocity of the flexural waves of high frequency. In this case, only the nonlocal elastic Timoshenko beam well predicts the flexural wave dispersion.

ACKNOWLEDGMENTS

Both authors greatly appreciate the valuable help of Professor Wanlin Guo and the financial support of The Innovation Fund for Graduate Students granted by Jiangsu Provincial Government, China.

APPENDIX: CONSTITUTIVE LAW OF HIGHER-ORDER-STRAIN-GRADIENT FOR A DISCRETE MEDIUM[19]

The appendix presents the model of higher-order strain-gradient by means of homogenization of the displacement field of a discrete medium. As shown in Fig. 5, the discrete medium consists of an infinite number of identical particles of mass m and identical springs of stiffness K and length d. It is easy to establish the dynamic equation for an arbitrary particle n as follows

$$m\ddot{u}_n + K(2u_n - u_{n+1} - u_{n-1}) = 0, \quad n = 1,2,\ldots . \tag{A1}$$

The homogenization procedure enables one to assume that the continuous displacement u is equal to the discrete displacement u_n at particle n. Then, the Taylor series gives the displacement at the neighboring particles

$$u_{n\pm1} = u_n \pm d\frac{\partial u_n}{\partial x_n} + \frac{d^2}{2}\frac{\partial^2 u_n}{\partial x_n^2} \pm \frac{d^3}{6}\frac{\partial^3 u_n}{\partial x_n^3} + \frac{d^4}{24}\frac{\partial^4 u_n}{\partial x_n^4} + \cdots . \tag{A2}$$

If the displacements of the discrete medium u_{n+1} and u_{n-1} are written in terms of the continuous displacement and are substituted into Eq. (A1), one arrives at

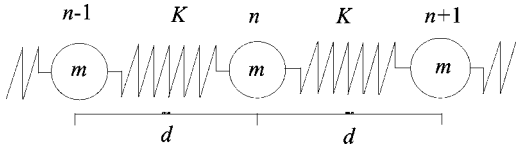

FIG. 5. The structure of the discrete medium.

$$\rho\ddot{u} = E\left(\frac{\partial^2 u}{\partial x^2} + \frac{1}{12}d^2\frac{\partial^4 u}{\partial x^4} + \frac{1}{360}d^4\frac{\partial^6 u}{\partial x^6} + \cdots\right), \quad \text{(A3)}$$

where $\rho = m/Ad$ is the mass density and $E = Kd/A$ is Young's modulus, where A represents the cross-section area of the beam. It is quite interesting that all the derivatives of odd orders can be automatically cancelled in Eq. (A3). When the kinematics relation $\varepsilon = \partial u/\partial x$ is used and the dynamic equation of the continuum is expressed as $\rho\ddot{u} = \partial\sigma/\partial x$, Eq. (A3) becomes the following constitutive law of the discrete medium

$$\sigma = E\left(\varepsilon + \frac{1}{12}d^2\frac{\partial^2 \varepsilon}{\partial x^2} + \frac{1}{360}d^4\frac{\partial^4 \varepsilon}{\partial x^4} + \cdots\right). \quad \text{(A4)}$$

Truncating Eq. (A4) at the second-order gradient yields Eq. (2), where $r = d/\sqrt{12}$.

*Corresponding author. Email address: hyhu@nuaa.edu.cn

[1] S. Iijima, Nature (London) **354**, 56 (1991).
[2] M. M. J. Treacy, T. W. Ebbesen, and J. M. Gibson, Nature (London) **381**, 678 (1996).
[3] O. Lourie and H. D. Wagner, J. Mater. Res. **13**, 2418 (1998).
[4] J. Bernholic, C. Brabec, M. Buongiorno Nardelli, A. Maiti, C. Roland, and B. I. Yakobson, Appl. Phys. A: Mater. Sci. Process. **67**, 39 (1998).
[5] N. Yao and V. Lordi, J. Appl. Phys. **84**, 1939 (1998).
[6] N. Yao and V. Lordi, Phys. Rev. B **58**, 12649 (1998).
[7] B. I. Yakobson, C. J. Brabec, and J. Bernholc, Phys. Rev. Lett. **76**, 2511 (1996).
[8] B. I. Yakobson, M. P. Campbell, C. J. Brabec, and J. Bernholc, Comput. Mater. Sci. **8**, 341 (1997).
[9] P. Zhang, P. E. Lammert, and V. H. Crespi, Phys. Rev. Lett. **81**, 5346 (1998).
[10] E. W. Wong, P. E. Sheehan, and C. M. Lieber, Science **277**, 1971 (1997).
[11] L. J. Sudak, J. Appl. Phys. **94**, 7281 (2003).
[12] Y. Q. Zhang, G. R. Liu, and J. S. Wang, Phys. Rev. B **70**, 205430 (2004).
[13] P. Poncharal, Z. L. Wang, D. Ugarte, and W. A. de Heer, Science **283**, 1513 (1999).
[14] J. Yoon, C. Q. Ru, and A. Mioduchowski, Phys. Rev. B **66**, 233402 (2002).
[15] J. Yoon, C. Q. Ru, and A. Mioduchowski, Compos. Sci. Technol. **63**, 1533 (2003).
[16] V. N. Popov, V. E. Van Doren, and M. Balkanski, Phys. Rev. B **61**, 3078 (2000).
[17] J. Yoon, C. Q. Ru, and A. Mioduchowski, J. Appl. Phys. **93**, 4801 (2003).
[18] J. Yoon, C. Q. Ru, and A. Mioduchowski, Composites, Part B **35**, 87 (2004).
[19] H. Askes, A. S. J. Suiker, and L. J. Sluys, Arch. Appl. Mech. **72**, 171 (2002).
[20] S. Timoshenko and J. Gere, *Mechanics of Materials* (Van Nostrand Reinhold, New York, 1972).
[21] R. R. Craig, Jr., *Structural Dynamics* (Wiley, New York, 1981).
[22] D. W. Brenner, Phys. Rev. B **42**, 9458 (1990).
[23] C. F. Cornwell and L. T. Wille, Solid State Commun. **101**, 555 (1997).
[24] T. Halicioglu, Thin Solid Films **312**, 11 (1998).
[25] P. Zhang, Y. Huang, P. H. Geubelle, P. A. Klein, and K. C. Hwang, Int. J. Solids Struct. **39**, 3893 (2002).